Diffusion in a potential landscape with stochastic resetting

Arnab Pal

Raman Research Institute, Bangalore 560080, India

The steady state of a Brownian particle diffusing in an arbitrary potential under the stochastic resetting mechanism has been studied. We show that there are different classes of nonequilibrium steady states depending on the nature of the potential. In the stable potential landscape, the system attains a well-defined steady state; however, the existence of the steady state for the unstable landscape is constrained. We have also investigated the transient properties of the propagator towards the steady state under the stochastic resetting mechanism. Finally, we have done numerical simulations to verify our analytical results.

PACS number(s): 05.40.−a

I. INTRODUCTION

Diffusion with stochastic resetting is considered to be a natural framework for the study of intermittent search processes [1,2]. The simplest question of finding a lost object, such as a key, a car, or an offender, is one of the central quests of the discipline. The search processes related to resetting are realized in diverse fields such as biochemistry (where a signaling molecule is reset back to a receptor protein in the membrane depending on the concentration of certain molecules in the vicinity) [3], computer networks (to find an element in a sorted and pivoted array) [4], ecology (e.g., Capuchin monkeys, known for long-term memory, foraging a territory with palm nuts) [5], and microbiology [6]. In addition, this mechanism was considered to compute the stationary distribution of variant models of population growth where the population is stochastically reset to some higher or lower values leading to a power law growth [7,8]. Also, there has been interest in studying the continuous time random walk, where both the position and the waiting time are chosen from certain distributions in the presence of resetting [9].

"Stochastic resetting" is a mechanism where a Brownian particle is stochastically reset to its initial position at a constant rate, thus driving the system away from any equilibrium state [10–13]. It is thus a simple mechanism to generate a nonequilibrium stationary state. In such states, probability currents are nonzero and the detailed balance does not hold naturally. Of late, the implication of the stochastic reset has been studied in the one-dimensional reaction-diffusion systems, where a finite reset rate leads to an unique nonequilibrium stationary state [14]. The interface growth models described by Kardar-Parisi-Zhang and Edwards-Wilkinson equations also exhibit nonequilibrium stationary states with non-Gaussian interface fluctuations when the interface stochastically resets to a fixed initial profile at a constant rate [15]. In this backdrop, a natural question to ask would be the following: Is the nonequilibrium stationary state generic to any dynamics subjected to stochastic resetting? The primary goal of this paper is to address this question. To gain insight, one considers model systems which are simple enough yet address the basic principle. In this paper, we consider a simple model of a Brownian particle diffusing in an arbitrary potential landscape in the presence of stochastic resetting. It is obvious that for a bounded case, even without reset, one gets a steady state around the minimum of the potential. But when the equilibrium point of the potential

differs from the reset point, two mechanisms compete with each other and finally reach a steady state, which shows certain generic behavior. On the other hand, for a particle diffusing in an unbounded potential, there exists no steady state at all in the absence of resetting. We propose to invoke stochastic resetting to retrieve the steady state. However, this behavior is not universal and rather puts a general constraint on the nature of the potential. We derive the conditions that ensure the steady state in the case of an unbounded potential.

The paper is structured as follows. In the following section, we introduce the model and the resetting dynamics. In Sec. III, we obtain the exact steady state distribution $P_{st}(x|x_0)$ for two representative choices of the potential $V(x)$, namely, (i) $V(x) \sim \mu|x|$ and (ii) $V(x) \sim \mu x^2$. The positive and negative sign of μ describe the bounded and unbounded potential, respectively. We also derive the conditions to obtain a unique steady state for an arbitrary potential landscape. In Sec. IV, we investigate the transient behavior of the propagator in the presence of the resetting. We conclude with a summary and future directions in Sec. V.

II. THE MODEL

Consider a single particle undergoing diffusion in one dimension in the presence of an external potential $V(x)$:

$$\frac{dx}{dt} = -V'(x) + \eta(t), \qquad (1)$$

where $\eta(t)$ is a Gaussian white noise with

$$\langle \eta(t) \rangle = 0, \quad \langle \eta(t)\eta(t') \rangle = 2D\delta(t - t'), \qquad (2)$$

and D is the diffusion constant and the viscosity of the medium has been scaled to unity for brevity. Here, angular brackets denote averaging over noise realizations. The initial condition is

$$x(0) = x_0, \qquad (3)$$

where $x_0 \in (0, \infty)$. We now introduce the "stochastic resetting" mechanism by which the particle returns to its initial location at a constant rate r. To elaborate, in a small time Δt, the particle is reset to the initial position $x = x_0$ with probability $r\Delta t$, while with the complementary probability $1 - r\Delta t$, the particle dynamics follows Eq. (1).

III. STEADY STATE DISTRIBUTION

Let $P(x,t|x_0)$ be the probability to find the particle at position x at time t, given that it was at x_0 at time $t = 0$. From the dynamical rules for the evolution of the particle given in the preceding section, it follows that

$$\frac{\partial P}{\partial t} = D\frac{\partial^2 P}{\partial x^2} + \frac{\partial [V'(x)P]}{\partial x} - rP + r\delta(x - x_0), \quad (4)$$

with the initial condition $P(x,0|x_0) = \delta(x - x_0)$. Here, the third and fourth terms on the right hand side (rhs) account for the resetting events, denoting the negative probability flux $-rP$ from each point x and a corresponding positive probability flux into $x = x_0$. The steady state solution $P_{st}(x|x_0)$ satisfies

$$0 = D\frac{d^2 P_{st}}{dx^2} + \frac{d[V'(x)P_{st}]}{dx} - rP_{st} + r\delta(x - x_0). \quad (5)$$

In the following section, we have investigated steady state distributions for various bounded and unbounded potential landscapes. In particular, we have studied two representative choices of the potential $V(x)$, namely, (i) $V(x) \sim \mu|x|$ and (ii) $V(x) \sim \mu x^2$.

A. The case of a mod potential

We first consider the case of a mod potential. This potential is centered either around its minimum or the maximum at 0. The reset location is at $x_0 \neq 0$. The nature of the potential allows us to identify three regions in x, namely, region I ($x > x_0$), region II ($0 < x < x_0$), and region III ($x < 0$). To find the steady state, we solve Eq. (5) in each region and require that the solutions are continuous at $x = x_0$, and $x = 0$ for a probability distribution representing a physical observable should be single valued everywhere in the phase space. This is also required to ascertain a finite diffusive current in the model system. However, the derivatives are discontinuous and it can be seen by integrating Eq. (5) over an infinitesimal region around $x = x_0$,

$$\left.\frac{dP_{st}^I(x|x_0)}{dx}\right|_{x=x_0} - \left.\frac{dP_{st}^{II}(x|x_0)}{dx}\right|_{x=x_0} = -\frac{r}{D}. \quad (6)$$

This discontinuity does not depend on μ, indicating the robustness of "kinks" present at x_0 irrespective of potential

landscapes. On the other hand, while integrating Eq. (5) over an infinitesimal region around $x = 0$, we find that

$$\left.\frac{dP_{st}^{II}(x|x_0)}{dx}\right|_{x=0} - \left.\frac{dP_{st}^{III}(x|x_0)}{dx}\right|_{x=0} = \mp\frac{2\mu}{D}P_{st}^{II}(x|x_0)\bigg|_{x=0}, \quad (7)$$

in which minus and plus signs are for the bounded and the unbounded case, respectively. In the following sections, we consider these two cases, respectively.

1. Bounded potential: $V(x) = \mu|x|, \mu > 0$

We first consider the case where $\mu > 0$. The trial solutions of Eq. (5) are of the form

$$P_{st}^I(x|x_0) = a_1 e^{m_1 x} + a_2 e^{m_2 x},$$
$$P_{st}^{II}(x|x_0) = b_1 e^{m_1 x} + b_2 e^{m_2 x}, \quad (8)$$
$$P_{st}^{III}(x|x_0) = c_1 e^{-m_1 x} + c_2 e^{-m_2 x},$$

where

$$m_1 = \frac{-\mu + \sqrt{\mu^2 + 4Dr}}{2D}, \quad m_2 = -\frac{\mu + \sqrt{\mu^2 + 4Dr}}{2D}. \quad (9)$$

Since the probabilities should converge at $x \to \pm\infty$, we have $a_1 = c_1 = 0$. Finally, using Eqs. (6) and (7), we obtain the steady state solutions given by

$$P_{st}^I(x|x_0) = \frac{r}{\sqrt{\mu^2 + 4Dr}} e^{-m_2 x_0} e^{m_2 x}$$
$$\qquad + \frac{\mu r}{\sqrt{\mu^2 + 4Dr}(\sqrt{\mu^2 + 4Dr} - \mu)} e^{-m_1 x_0} e^{m_2 x},$$

$$P_{st}^{II}(x|x_0) = \frac{r}{\sqrt{\mu^2 + 4Dr}} e^{-m_1 x_0} e^{m_1 x}$$
$$\qquad + \frac{\mu r}{\sqrt{\mu^2 + 4Dr}(\sqrt{\mu^2 + 4Dr} - \mu)} e^{-m_1 x_0} e^{m_2 x},$$

$$P_{st}^{III}(x|x_0) = \frac{r}{\sqrt{\mu^2 + 4Dr} - \mu} e^{-m_1 x_0} e^{-m_2 x}. \quad (10)$$

Figure 1 shows a comparison between simulations and theory for the steady state given by Eq. (10), demonstrating a very good agreement. From the solution, it is evident that
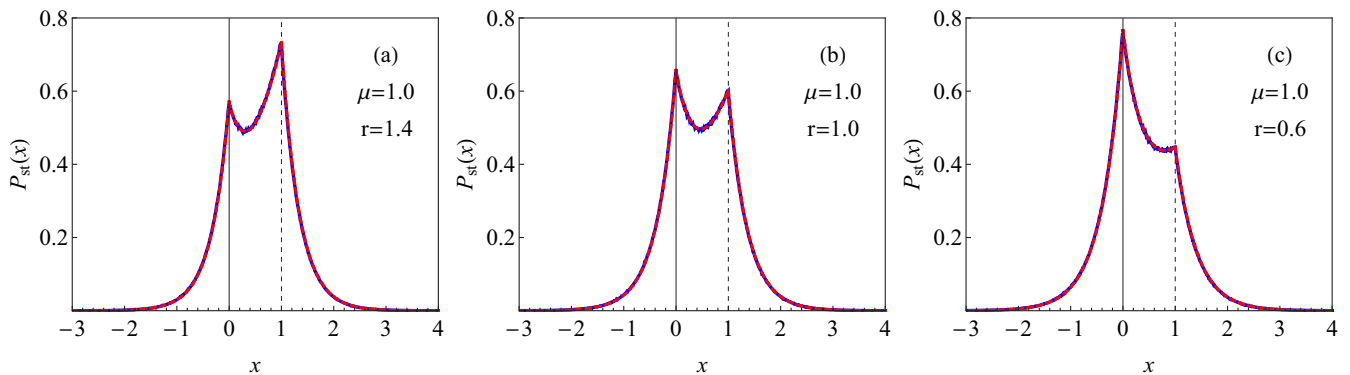
FIG. 1. (Color online) Stationary distribution $P_{st}(x|x_0)$ for the bounded potential $V(x) = \mu|x|$, with $\mu > 0$. We choose $D = 0.5, x_0 = 1.0, \mu = 1.0$, while r varies. The (red) dashed line plots the analytical result for $P_{st}(x)$, while the (blue) points are numerical simulation results. Also, the vertical solid and dashed lines indicate the location of the stable minimum of the bounded potential and the reset point x_0, respectively. The motion of the peak is also clear from the figure.
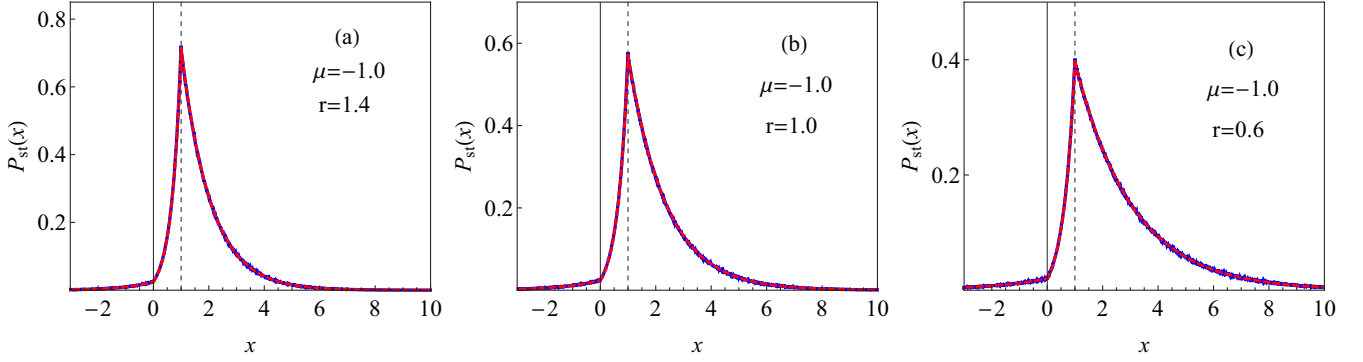
FIG. 2. (Color online) Stationary distribution $P_{st}(x|x_0)$ for the unbounded potential $V(x) = \mu|x|$, with $\mu < 0$. We choose $D = 0.5$, $x_0 = 1.0, \mu = -1.0$, while r varies. The (red) dashed line plots the analytical result for $P_{st}(x)$, while the (blue) points are numerical simulation results. Also, the vertical solid and dashed lines indicate the location of the unstable maximum of the unbounded potential and the reset point x_0, respectively.

$P_{st}(x|x_0)$ exhibits two cusps where its derivatives are discontinuous, namely, (i) at the resetting location $x = x_0$, and (ii) at $x = 0$, the point at which the potential $V(x)$ has discontinuous derivatives.

2. Unbounded potential: $V(x) = \mu|x|, \mu < 0$

Following the similar structure as before and using the matching conditions suitably, we obtain the steady state solutions for the unbounded case when $\mu < 0$ to be

$$P_{st}^{I}(x|x_0) = \frac{r}{\sqrt{\mu^2 + 4Dr}}e^{m_1 x_0}e^{-m_1 x} - \frac{\mu r}{\sqrt{\mu^2 + 4Dr}(\sqrt{\mu^2 + 4Dr} + \mu)}e^{m_2 x_0}e^{-m_1 x},$$

$$P_{st}^{II}(x|x_0) = \frac{r}{\sqrt{\mu^2 + 4Dr}}e^{m_2 x_0}e^{-m_2 x} - \frac{\mu r}{\sqrt{\mu^2 + 4Dr}(\sqrt{\mu^2 + 4Dr} + \mu)}e^{m_2 x_0}e^{-m_1 x}, \qquad (11)$$

$$P_{st}^{III}(x|x_0) = \frac{r}{\sqrt{\mu^2 + 4Dr} + \mu}e^{m_2 x_0}e^{m_1 x},$$

where m_1, m_2 are given by Eq. (9).

Figure 2 shows a comparison between simulations and theory for the steady state given by Eq. (11), demonstrating a very good agreement. Again, $P_{st}(x|x_0)$ exhibits two cusps where its derivatives are discontinuous, namely, (i) at the resetting location $x = x_0$, and (ii) at $x = 0$, the point at which the potential $V(x)$ has discontinuous derivatives.

3. Numerical simulations

The probability distribution function $P_{st}(x|x_0)$ can be computed using the basic Langevin dynamics techniques. The dynamical rule for the resetting process is given by

$$x(t + \Delta t) = \begin{cases} x_0, & \text{with probability } r\Delta t \\ x(t) + f(x(t))\Delta t + \sqrt{2D\Delta t}\, y, & \text{with probability } (1 - r\Delta t), \end{cases} \qquad (12)$$

where the force is $f(x) = -V'(x) = -\mu \text{sgn}(x)$, Δt is the infinitesimal time step chosen *a priori*, and y is a zero mean, unit variance Gaussian random variable. So, at each time step Δt, the particle either gets reset at x_0 with probability $r\Delta t$ or undergoes a Brownian dynamics with probability $1 - r\Delta t$. In this way, one will have a time series of the particle's position until time t and thus one can compute the position distribution function of the particle over many realizations starting from the same initial condition, $x(0) = x_0$. The particle eventually attains its steady state and we can compute the steady state distribution from the data.

B. The case of a quadratic potential

We now consider the case of a harmonic potential centered around 0 which is either its minimum or the maximum. As

before, reset takes place at x_0. One can again identify two regions in x, namely, region I ($x > x_0$) and region II ($x < x_0$). We solve Eq. (5) in each region and use the fact that the solutions are continuous at $x = x_0$ while the derivatives are not. This can be seen by integrating Eq. (5) over an infinitesimal region around $x = x_0$, where one finds

$$\frac{dP_{st}^{I}(x|x_0)}{dx}\bigg|_{x=x_0} - \frac{dP_{st}^{II}(x|x_0)}{dx}\bigg|_{x=x_0} = -\frac{r}{D}. \qquad (13)$$

This is consistent with the fact mentioned in Eq. (6). Similar to the last section, in the following we derive the steady state solutions for both the stable and the unstable landscape.

1. Bounded potential: $V(x) = (\mu/2)x^2$

We first consider the case where $\mu > 0$ and this is the case of a bounded harmonic potential. The solutions are then given by

$$
\begin{aligned}
P_{st}^{I}(x|x_0) &= c_1 e^{-\frac{\mu}{2D}x^2} H\left(-\frac{r}{\mu}, \sqrt{\frac{\mu}{2D}}x\right) \\
&\quad + c_2 e^{-\frac{\mu}{2D}x^2} {}_1F_1\left(\frac{r}{2\mu}; \frac{1}{2}; \frac{\mu}{2D}x^2\right), \\
P_{st}^{II}(x|x_0) &= c_3 e^{-\frac{\mu}{2D}x^2} H\left(-\frac{r}{\mu}, \sqrt{\frac{\mu}{2D}}x\right) \\
&\quad + c_4 e^{-\frac{\mu}{2D}x^2} {}_1F_1\left(\frac{r}{2\mu}; \frac{1}{2}; \frac{\mu}{2D}x^2\right),
\end{aligned}
\tag{14}
$$

where $H(-n,x)$ is the Hermite polynomial of negative order n [16], and ${}_1F_1(a;b;x)$ is the Kummer confluent hypergeometric function. We note that $H(-n,\sqrt{\mu}x)$ converges as x^{-n} when $x \to \infty$ but diverges as $x^{n-1}e^{\mu x^2}$ when $x \to -\infty$. But ${}_1F_1(a;b;\mu x^2)$ is even in x and diverges as $e^{\mu x^2}x^{a-b}$ when $x \to \pm\infty$. However, these functions are multiplied with $e^{-\mu x^2}$ and then the exponentials cancel each other which makes the additional algebraic form important at the asymptotic limits. This results in two distinct situations, namely, $r \geqslant \mu$ and $r < \mu$. In the first case, one needs to choose $c_2 = 0$ for the convergence of the steady state. However, in the second case, one can show that it is not necessary to choose $c_2 = 0$, rather there are infinite choices for c_2 and, for each, c_1 will be automatically determined by the normalization condition. In this paper, we choose $c_2 = 0$ to maintain an identical structure between the two cases. Using the matching conditions given by Eq. (13), we obtain

$$
\begin{aligned}
c_1 H\left(-\frac{r}{\mu}, \sqrt{\frac{\mu}{2D}}x_0\right) &= c_3 H\left(-\frac{r}{\mu}, \sqrt{\frac{\mu}{2D}}x_0\right) \\
&\quad + c_4 {}_1F_1\left(\frac{r}{2\mu}; \frac{1}{2}; \frac{\mu}{2D}x_0^2\right),
\end{aligned}
\tag{15}
$$

and

$$
\begin{aligned}
\frac{c_1}{\sqrt{\mu}} &H\left(-1-\frac{r}{\mu}, \sqrt{\frac{\mu}{2D}}x_0\right) \\
&= \frac{c_3}{\sqrt{\mu}} H\left(-1-\frac{r}{\mu}, \sqrt{\frac{\mu}{2D}}x_0\right) \\
&\quad - \frac{c_4 x_0}{\sqrt{2D}} {}_1F_1\left(1+\frac{r}{2\mu}; \frac{3}{2}; \frac{\mu}{2D}x_0^2\right) + \frac{1}{\sqrt{2D}}e^{\frac{\mu}{2D}x_0^2}.
\end{aligned}
\tag{16}
$$

For further analysis, let us choose $D = 1/2$, without loss of generality. It is convenient to define the following quantities:

$$
\begin{aligned}
z_1(r,\mu,x_0) &\equiv \sqrt{\mu}x_0 H\left(-\frac{r}{\mu}, \sqrt{\mu}x_0\right) {}_1F_1\left(1+\frac{r}{2\mu}; \frac{3}{2}; \mu x_0^2\right) \\
&\quad + H\left(-1-\frac{r}{\mu}, \sqrt{\mu}x_0\right) {}_1F_1\left(\frac{r}{2\mu}; \frac{1}{2}; \mu x_0^2\right),
\end{aligned}
\tag{17}
$$

$$
a_1(r,\mu,x_0) \equiv \sqrt{\mu}e^{\mu x_0^2} {}_1F_1\left(\frac{r}{2\mu}; \frac{1}{2}; \mu x_0^2\right),
\tag{18}
$$

$$
b_1(r,\mu,x_0) \equiv \sqrt{\mu}e^{\mu x_0^2} H\left(-\frac{r}{\mu}, \sqrt{\mu}x_0\right).
\tag{19}
$$

Using these definitions and from Eqs. (15) and (16), we obtain

$$
c_3 = c_1 - \frac{a_1(r,\mu,x_0)}{z_1(r,\mu,x_0)},
\tag{20}
$$

$$
c_4 = \frac{b_1(r,\mu,x_0)}{z_1(r,\mu,x_0)}.
\tag{21}
$$

Thus, c_4 is independent of c_1, while c_3 depends on c_1 and can be evaluated once c_1 is found from the normalization condition,

$$
\int_{-\infty}^{x_0} dx\, P_{st}^{II}(x|x_0) + \int_{x_0}^{\infty} dx\, P_{st}^{I}(x|x_0) = 1.
\tag{22}
$$

That said, one obtains the full steady state solutions from Eq. (14).

Figure 3 shows a comparison between simulations, as described in Sec. III A 3, and theory for the steady state (14),
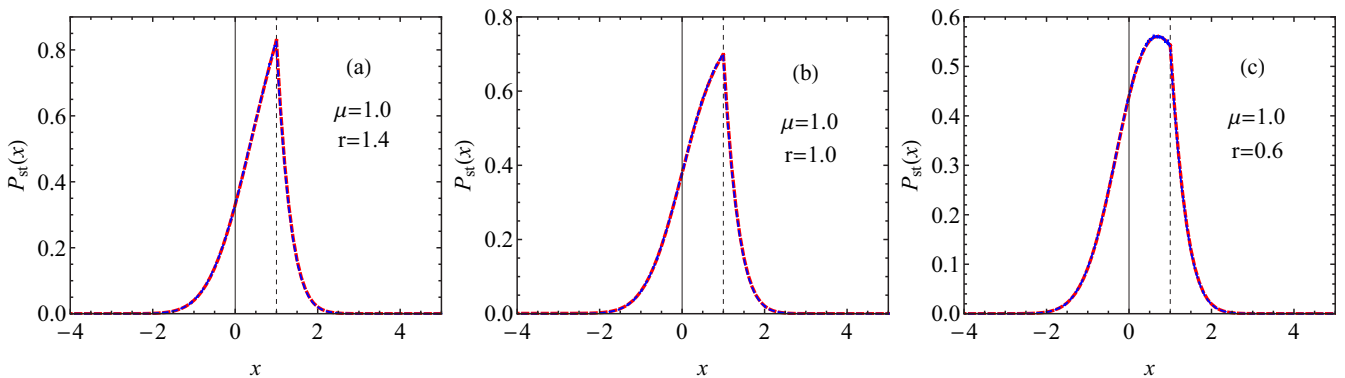
FIG. 3. (Color online) Stationary distribution $P_{st}(x)$ for the potential $V(x) = (\mu/2)x^2$, with $\mu > 0$. We choose $D = 0.5$, $x_0 = 1.0$, $\mu = 1.0$, while r varies. The (red) dashed line plots the analytical result for $P_{st}(x)$, while the (blue) points are numerical simulation results. The vertical solid and dashed lines indicate the location of the stable minimum of the bounded potential and the reset point x_0, respectively. The motion of the peak is also clear from the figure.

demonstrating a very good agreement. We note that there is only a cusp at the reset point $x = x_0$. When r is large compared to μ, the distribution is peaked around $x = x_0$ with a non-Gaussian form. However, when μ is much greater than r, we get a distribution peaked around the minimum of the potential. In between, the peak moves between x_0 and the minimum. This generic feature of the distribution is clear from Fig. 3.

2. Unbounded potential: $V(x) = -(\mu/2)x^2$

We proceed further with a similar analysis in the case of the unbounded harmonic potential and the solutions are given by

$$P_{st}^I(x|x_0) = d_1 H\left(-1 - \frac{r}{\mu}, \sqrt{\frac{\mu}{2D}}x\right),$$

$$P_{st}^{II}(x|x_0) = d_3 H\left(-1 - \frac{r}{\mu}, \sqrt{\frac{\mu}{2D}}x\right) \tag{23}$$

$$+ d_4\, {}_1F_1\left(\frac{1}{2} + \frac{r}{2\mu}; \frac{1}{2}; \frac{\mu}{2D}x^2\right),$$

where $H(-n,x)$ is the Hermite polynomial of negative order n, and ${}_1F_1(a;b;x)$ is the Kummer confluent hypergeometric function, which is the same as before. Using the matching conditions given by Eq. (13) in this case, we obtain

$$d_1 H\left(-1 - \frac{r}{\mu}, \sqrt{\frac{\mu}{2D}}x_0\right) = d_3 H\left(-1 - \frac{r}{\mu}, \sqrt{\frac{\mu}{2D}}x_0\right)$$

$$+ d_4\, {}_1F_1\left(\frac{1}{2} + \frac{r}{2\mu}; \frac{1}{2}; \frac{\mu}{2D}x_0^2\right), \tag{24}$$

and

$$d_1 H\left(-2 - \frac{r}{\mu}, \sqrt{\frac{\mu}{2D}}x_0\right)$$

$$= d_3 H\left(-2 - \frac{r}{\mu}, \sqrt{\frac{\mu}{2D}}x_0\right)$$

$$- d_4 \sqrt{\frac{\mu}{2D}}x_0\, {}_1F_1\left(\frac{3}{2} + \frac{r}{2\mu}; \frac{3}{2}; \frac{\mu}{2D}x_0^2\right)$$

$$+ \frac{r}{\sqrt{2D\mu}}\left(1 + \frac{r}{\mu}\right)^{-1}. \tag{25}$$

Choosing $D = 1/2$ and using Eqs. (24) and (25), one obtains

$$d_3 = d_1 - \frac{a_2(r,\mu,x_0)}{z_2(r,\mu,x_0)}, \tag{26}$$

$$d_4 = \frac{b_2(r,\mu,x_0)}{z_2(r,\mu,x_0)}, \tag{27}$$

where

$$z_2(r,\mu,x_0) \equiv (r+\mu)\left[\sqrt{\mu}x_0 H\left(-1 - \frac{r}{\mu}, \sqrt{\mu}x_0\right)\right.$$

$$\times {}_1F_1\left(\frac{3}{2} + \frac{r}{2\mu}; \frac{3}{2}; \mu x_0^2\right)$$

$$\left. + H\left(-2 - \frac{r}{\mu}, \sqrt{\mu}x_0\right){}_1F_1\left(\frac{1}{2} + \frac{r}{2\mu}; \frac{1}{2}; \mu x_0^2\right)\right], \tag{28}$$

$$a_2(r,\mu,x_0) \equiv r\sqrt{\mu}\, {}_1F_1\left(\frac{1}{2} + \frac{r}{2\mu}; \frac{1}{2}; \mu x_0^2\right), \tag{29}$$

$$b_2(r,\mu,x_0) \equiv r\sqrt{\mu} H\left(-1 - \frac{r}{\mu}, \sqrt{\mu}x_0\right). \tag{30}$$

Then d_1 can be found using the normalization condition given by Eq. (22) as before and the solutions are deduced from Eq. (23).

Figure 4 shows a comparison between simulations and theory for the steady state given by Eq. (23), demonstrating a very good agreement. We note that there is only a cusp at the reset point $x = x_0$. When r is large compared to μ, the distribution is peaked around $x = x_0$ with a non-Gaussian form. However, when μ is much greater than r, the peak does not move, unlike the case of the bounded potential. Nevertheless, in this limit, the system takes longer time to reach the steady state with a peak well set at $x = x_0$, indicating a fat tailed distribution at large x [17]. We refer to Fig. 4 which characterizes this generic feature.

C. General $V(x)$: Possible steady states

We generalize our discussion for arbitrary potential that has a form $V(x) = \mu|x|^\delta$. When $\mu > 0$, that is, the potential is stable with minimum at $x = x_{min}$, one will always achieve
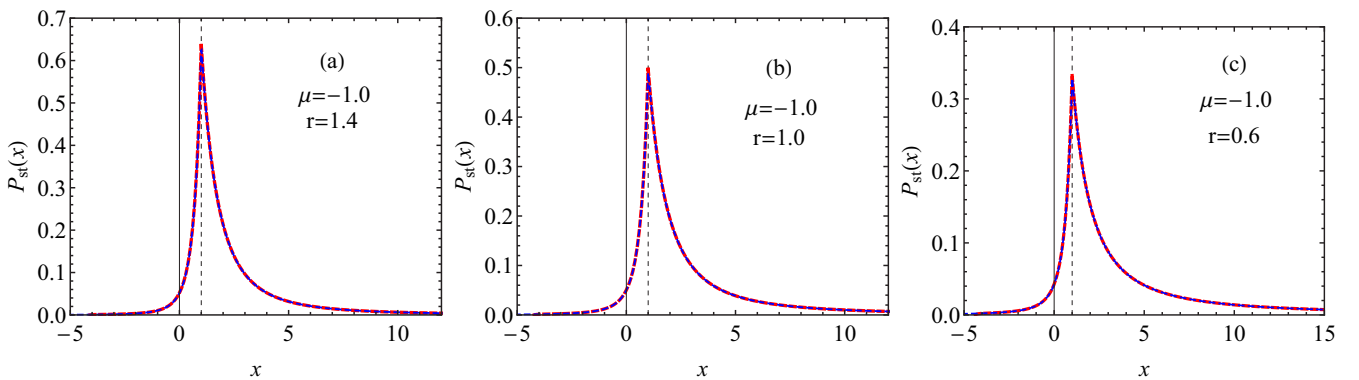
FIG. 4. (Color online) Stationary distribution $P_{st}(x)$ for the potential $V(x) = (\mu/2)x^2$, with $\mu < 0$. We choose $D = 0.5$, $x_0 = 1.0$, $\mu = -1.0$ while r varies. The (red) dashed line plots the analytical result for $P_{st}(x)$, while the (blue) points are numerical simulation results. The vertical solid and dashed lines indicate the location of the unstable maximum of the unbounded potential and the reset point x_0, respectively.

the steady state around $x_{\min}$, irrespective of the resetting. Nevertheless, resetting will invoke the nondifferentiability in the steady state, resulting in a cusp at the reset point $x_0 \neq x_{\min}$. Here one can talk about two extreme limits: one is when the strength of the potential is much greater than the reset rate and one expects a steady state solution of form $\sim e^{-V(x)}$ centered around $x_{\min}$ with a small but nonvanishing cusp at x_0, given by Eq. (6). In the other limit, when the reset rate dominates the potential strength, one finds a non-Gaussian form around x_0. However, in between, the peak of the steady state moves from $x_{\min}$ to x_0 as one varies r but keeps μ fixed. This is a generic feature that can be seen for any δ.

Now consider the case when $\mu < 0$. There is no stable minimum of the potential, hence no steady state since the particle escapes to infinity in the absence of stochastic resetting. However, we notice that one can have a steady state when resetting is introduced under certain conditions, which we discuss in the following. We can find a steady state if and only if $V(x)$ is such that the particle starting from x_0 does not escape to infinity at a finite time in the absence of resetting. Note that the escape time is given by $t_{\mathrm{esc}} = -\int_{x_0}^{\infty} [V'(x)]^{-1} dx = [x_0^{\delta-2}(\delta-2)\delta\mu]^{-1}$ for $\delta > 2$. On the other hand, the waiting time distribution for resetting is given by Poisson distribution, namely, $re^{-r\tau}$, where the average time between two resets is simply given by $t_{\mathrm{reset}} = 1/r$, which is always finite. It is then obvious that if $t_{\mathrm{esc}} < t_{\mathrm{reset}}$, the particle always escapes and there is no steady state. However, one indeed achieves a steady state if $t_{\mathrm{esc}} > t_{\mathrm{reset}}$, even for $\delta > 2$. This can be realized by increasing the reset rate so that it gets reset promptly before escaping. On the contrary, for $\delta \leqslant 2$, one finds $t_{\mathrm{esc}} \to \infty$, thus always maintaining a steady state through resetting. We have discussed the cases of $\delta = 2$ (harmonic) and $\delta = 1$ (mod) for both positive and negative μ in great detail. For positive μ, the steady states and the motion of the peak as well follow from Figs. 1(b) and 1(c) and Figs. 3(b) and 1(c). But for negative μ, the peak is always set at x_0, indicating the fact that the steady state is solely due to the reset mechanism. This is realized from Figs. 2 and 4.

IV. RELAXATION TO THE STEADY STATE

In this section, we investigate the transient behavior of the stochastic resetting mechanism. We recall that the particle starts at $x = x_0$ at $t = 0$ and finally attains a steady state either at $x = x_0$ or $x = x_{\min}$ as $t \to \infty$, depending on the potential landscape. In between, the position distribution function shows rich behavior which can be quantified by studying the relaxation dynamics of the propagator. We first recall Eq. (4),

$$\frac{\partial P}{\partial t} = D\frac{\partial^2 P}{\partial x^2} + \frac{\partial[V'(x)P]}{\partial x} - rP + r\delta(x - x_0), \quad (31)$$

with the boundary conditions $P(x \to \pm\infty, t) = 0$ and the initial condition $P(x, t = 0) = \delta(x - x_0)$. Now to characterize the transient states, one has to solve Eq. (4) for the time dependent propagator. To do this, we first separate $P(x,t) = f(x) + b(t,x)$, where $f(x)$ gives the steady state solution and $b(t,x)$ describes the relaxation towards it. As a representative case, we choose the free diffusion with no potential. The steady state solution $f(x)$ then satisfies the simple equation (5) with

the boundary conditions $f(x \to \pm\infty) = 0$,

$$Df''(x) - rf(x) + r\delta(x - x_0) = 0, \quad (32)$$

and this gives rise to the solution

$$f(x) = \frac{\alpha}{2}\exp[-\alpha|x - x_0|], \quad (33)$$

where $\alpha = \sqrt{\frac{r}{D}}$ is an inverse length scale denoting the typical distance diffused by the particle between the resets [10]. The time dependent part is given by

$$\partial_t b(t,x) = D\partial_x^2 b(t,x) - rb(t,x), \quad (34)$$

with the boundary conditions $b(t, x \to \pm\infty) = 0$ and $b(t \to \infty, x) \to 0$. The initial condition is given by $b_0(x) \equiv b(t = 0, x) = P(x,0) - f(x)$. This results in the complete form of
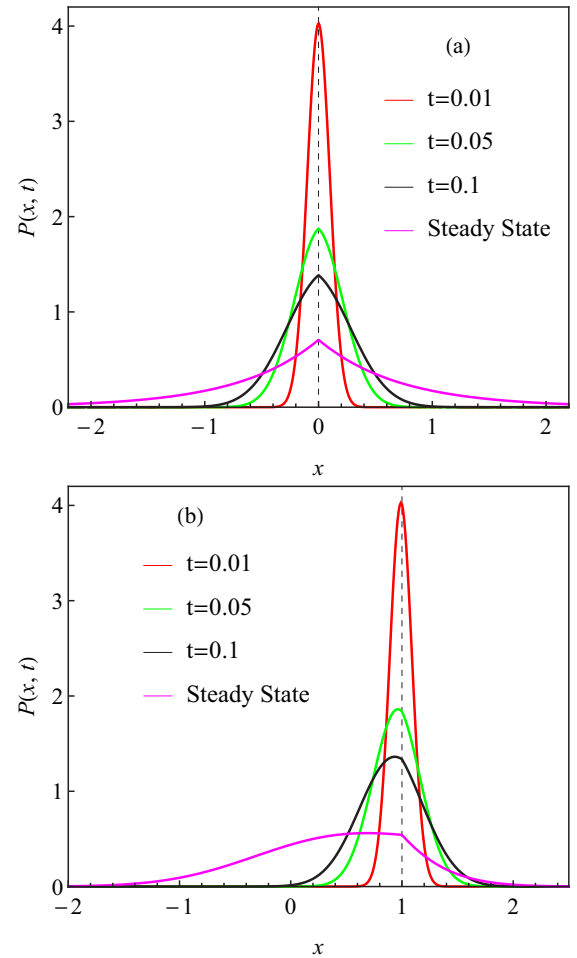
FIG. 5. (Color online) The time dependent propagator for the free and forced diffusion case in the presence of stochastic resetting has been plotted. It depicts the transient of the propagator from time zero to its steady state. Figures 5(a) and 5(b) represent the free and the forced diffusion cases respectively. The parameters are chosen to be $r = 0.6$, $\mu = 1.0$, and $D = 0.5$. The vertical dashed line marks the reset position x_0. In the free case (a), we consider $x_0 = 0$, but for the case (b), we set $x_0 = 1.0$, which is different from the stable minimum $x_{\min} = 0$.

the relaxation term given by

$$b(t,x) = e^{-rt} \frac{\exp\left[-\frac{(x-x_0)^2}{4Dt}\right]}{\sqrt{4\pi Dt}} - \frac{\alpha}{2}\cosh[-\alpha(x_0 - x)]$$
$$+ \frac{\alpha}{4}\exp[-\alpha(x_0 - x)]\mathrm{erf}\left[\frac{x - x_0 + 2Dt\alpha}{\sqrt{4\pi Dt}}\right]$$
$$+ \frac{\alpha}{4}\exp[\alpha(x_0 - x)]\mathrm{erf}\left[\frac{-x + x_0 + 2Dt\alpha}{\sqrt{4\pi Dt}}\right]. \quad (35)$$

Now, Eqs. (33) and (35) constitute the full propagator. We refer to Fig. 5(a), which specifies the relaxation for this particular case. A similar analysis can also be made for a Brownian particle diffusing in a potential in the presence of resetting. For instance, we analyze the case of a bounded harmonic potential $V(x) = (\mu/2)x^2$ with minimum $x_{\min} = 0$, while the reset point is at $x_0 \neq 0$. This gives rise to a competition between the potential and the reset mechanism, thus reaching a steady state as discussed in Sec. III C. Figure 5(b) characterizes the transient behavior with respect to t for $\mu = 1.0, r = 0.6$. We also notice that the steady state achieved at the end is identical to that obtained in Fig. 3(c).

V. SUMMARY

In this work, we have considered a Brownian particle diffusing in an arbitrary potential landscape in the presence of the stochastic resetting mechanism. We have investigated the steady state properties of the position distribution of the particle for two representative choices of the potential, namely, the mod and the harmonic potential. It has been shown that the steady states have distinct differences depending on the nature of the potential. We also derive the conditions for the existence of the steady state for any potential landscape of higher order. Also we have realized the transient behavior of the propagator approaching the steady state. We have studied two representative cases in this context, though the extension to higher order potential does not offer more physical insight.

Furthermore, resetting has been found to have a profound consequence on the first passage properties of a diffusing particle. In recent times, there have been extensive studies on this to have a discreet idea not only restricted to one dimension but to higher dimensions as well [18]. Consequently, the study of two observables, namely, the local time and the occupation time, turns out to be very useful to understand the mechanism near the reset point. Local time measures the time that the process visits a reference point (which is basically the reset point), while the residence time or the occupation time measures the time that the process stays above that point [19,20]. These observables show rich behavior when the resetting dynamics is combined [17]. There are many open questions in the context of the stochastic resetting mechanism. One can generalize resetting to the systems where the resetting takes place to a region instead of a reference point at a constant rate. Also, exploring the span or the extremum (namely, maximum or minimum) of a dynamics under the resetting paradigm will be very interesting in connection with the extreme value statistics [21].

[1] W. J. Bell, *Searching Behaviour: The Behavioural Ecology of Finding Resources* (Chapman and Hall, London, 1991).

[2] O. Benichou, C. Loverdo, M. Moreau, and R. Voituriez, Rev. Mod. Phys. **83**, 81 (2011).

[3] G. Adam and M. Delbruck, in *Structural Chemistry and Molecular Biology*, edited by A. Rich and N. Davidson (Freeman, San Francisco, 1968).

[4] A. Montanari and R. Zecchina, Phys. Rev. Lett. **88**, 178701 (2002).

[5] F. Bartumeus and J. Catalan, J. Phys. A: Math. Theor. **42**, 434002 (2009).

[6] M. E. Cates, Rep. Prog. Phys. **75**, 042601 (2012).

[7] S. C. Manrubia and D. H. Zanette, Phys. Rev. E **59**, 4945 (1999).

[8] P. Visco, R. J. Allen, S. N. Majumdar, and M. R. Evans, Biophys. J. **98**, 1099 (2010).

[9] M. Montero and J. Villarroel, Phys. Rev. E **87**, 012116 (2013).

[10] M. R. Evans and S. N. Majumdar, Phys. Rev. Lett. **106**, 160601 (2011).

[11] M. R. Evans and S. N. Majumdar, J. Phys. A: Math. Theor. **44**, 435001 (2011).

[12] M. R. Evans, S. N. Majumdar, and K. Mallick, J. Phys. A: Math. Theor. **46**, 185001 (2013).

[13] J. Whitehouse, M. R. Evans, and S. N. Majumdar, Phys. Rev. E **87**, 022118 (2013).

[14] X. Durang, M. Henkel, and H. Park, J. Phys. A: Math. Theor. **47**, 045002 (2014).

[15] S. Gupta, S. N. Majumdar, and G. Schehr, Phys. Rev. Lett. **112**, 220601 (2014).

[16] Computer code MATHEMATICA, Version 10.0 (Wolfram Research, Champaign, IL, 2014), Gradshteyn and Ryzhik, *Table of Integrals, Series, and Products*, 8th ed. (Academic, New York, 2014).

[17] A. Pal, P. Basu, and S. Gupta (unpublished).

[18] M. R. Evans and S. N. Majumdar, J. Phys. A: Math. Theor. **47**, 285001 (2014).

[19] S. N. Majumdar, Curr. Sci. **89**, 2076 (2005).

[20] S. Sabhapandit, S. N. Majumdar, and A. Comtet, Phys. Rev. E **73**, 051102 (2006).

[21] S. N. Majumdar and A. Pal, arXiv:1406.6768.